

1
2
3
4
5
6
7
8
9
10
11
12
13
14
15
16
17

Towards a crystal-clear view of the viral RNA sensing and response by RIG-I-like receptors

Dahai Luo ¹

¹Lee Kong Chian School of Medicine, Nanyang Technological University, Singapore 639798.

E-mail: luodahai@ntu.edu.sg

Running title: RNA recognition, ATP hydrolysis and Activation of RLRs

Keywords: innate immunity, helicase, signal transduction, virus infection, X-ray crystallography.

18 **Abstract**

19 The RIG-I-like receptors (RLRs) – RIG-I, MDA5, and LGP2 – detect intracellular
20 pathogenic RNA and elicit an antiviral immune response during viral infection. The protein
21 architecture of the RLR family consists of multiple functional domains, including N-terminal
22 Caspase Activation and Recruitment Domains (CARDs) for signaling initiation, a central RNA
23 helicase core and a C-terminal domain for RNA sensing. With these specialized sensing-and-
24 responding modules, RLRs are able to selectively bind non-self RNA species and trigger
25 downstream signaling events leading to interferon production. This article summarizes the recent
26 progress towards defining the precise mechanisms of RNA recognition and subsequent signal
27 induction by RLRs.

28

29 **RIG-I like receptors activate the antiviral immune response.**

30 Upon the breakage of the physical and chemical barriers - skin, mucous membranes,
31 body fluids, the immediate defense against pathogenic infections in our body is the innate
32 immune response. In our immune system, pattern recognition receptors (PRRs) are primarily
33 responsible for the detection of pathogens by recognizing pathogen associated molecular patterns
34 (PAMPs), pathogen-derived molecules that are different from those normally found in the host¹.
35 PAMPs are diverse in their origin, chemical and structural nature, and subcellular localization,
36 and therefore demand a broad spectrum of PRRs for their detection. Based on gene structure,
37 there are four major classes of PRRs: Toll-like-receptors (TLRs), nucleotide-binding
38 oligomerization domain receptors (NLRs), RIG-I-like-receptors (RLRs), and C-type lectin
39 receptors (CLRs)¹.

40 RLRs are specialized intracellular PRRs that detect pathogenic RNA species generated
41 during infection by viruses and other foreign organisms. There are three members of the RLR
42 family: retinoic acid-inducible gene 1 (RIG-I), melanoma differentiation-associated gene 5
43 (MDA5) and laboratory of genetics and physiology 2 (LGP2)². RIG-I and MDA5 are similar to
44 each other both structurally and functionally. Both contain two tandem caspase activation and
45 recruitment domains (CARDs; CARD1 and CARD2) at the N-terminus, which initiate a
46 downstream signaling relay; a central double-stranded RNA stimulated ATPase (DRA) motor
47 domain, and a C-terminal domain (CTD) that facilitates viral RNA recognition (**Fig 1**)³⁻⁷.
48 However, they have different preferences towards the RNA species they recognize; RIG-I
49 recognizes short, duplex RNA with a 5' end triphosphate, whereas longer and non-
50 triphosphorylated substrates are also able to efficiently activate RIG-I. In contrast, MDA5
51 cooperatively binds long duplex RNAs with no preference in 5' end character⁸. Therefore it is not
52 surprising that RIG-I and MDA5 recognize different but overlapping groups of RNA viruses².
53 LGP2 does not contain the N-terminal CARDs and is thought to serve as a feedback regulator.
54 However, the exact function and preferred RNA ligands of LGP2 are not clearly defined^{9, 10}.
55 RLRs are less abundant and remain inactive in resting cells. Detection and binding of viral RNA
56 stimulates the ATPase activity of RIG-I and MDA5 and initiates a signalling cascade leading to
57 type I interferon (IFN) production^{8, 11}. The adaptor protein for signal transduction is MAVS, also
58 known as IPS-1, VISA or CARDIF¹²⁻¹⁵, which is found on the outer mitochondrial membrane.
59 Activated RIG-I or MDA5 trigger MAVS oligomerization through their exposed CARDs. This
60 activation process is assisted by post-translational modifications like phosphorylation,
61 ubiquitination and non-covalent poly-ubiquitin binding^{16, 17}. Oligomeric MAVS then activates
62 several transcription factors – including IRF3, IRF7 and NF-κB – that induce the production of

63 type I IFN and inflammatory cytokines^{3, 18, 19}, which in turn help to engage the adaptive immune
64 system to eliminate the infection and build immunological memory²⁰. The molecular mechanism
65 of MAVS mediated IFN/Cytokine expression has been subjected to extensive study²¹. The latest
66 findings suggest that the activated MAVS is able to recruit and activate E3 ligases TRAF2,
67 TRAF5, and TRAF6 to ubiquitinate TRAF2 and other proteins, which then through the adaptor
68 NEMO recruit kinases -IKK and TBK1²². These kinases phosphorylate I κ B α and IRF3 and
69 therefore activate the transcription factors – IRF3 and NF- κ B – to switch on the gene expression
70 of IFN and cytokines^{11, 21, 22}.

71 As a subgroup of the Superfamily 2 (SF2) nucleic acid dependent ATPases, RLRs
72 contain a helicase core in the middle of the gene⁷. This core domain harbors the conserved
73 structural and functional elements of Superfamily 1 and 2 (SF1 and SF2) nucleic acid dependent
74 ATPases: two RecA-like domains containing a set of conserved sequence features: motifs Q, I,
75 II, and VI forms the ATP binding and hydrolysis pocket; motifs Ia, Ib, Ic, IV, IVa, V and Vb
76 mediate RNA binding; motifs III and Va coordinate nucleic acid binding with ATP hydrolysis
77 (**Fig 1F**)^{23, 24}. Despite these similarities, RLRs do not fall into the classical helicase category.
78 They thus belong to a subgroup of superfamily 2 RNA helicases, namely Duplex RNA-activated
79 ATPases (DRAs), which also include Dicer and Dicer-related helicases from worms⁷. As the
80 name implies, both the ATPase activity and subsequent cellular functions of these proteins are
81 stimulated by interaction with dsRNA (**Fig 2A**). Furthermore, DRAs do not appear to display
82 RNA unwinding activity. They lack the β -hairpin motif on the second helicase domain which has
83 been shown to be the duplex opener in the hel308 DNA helicase (**Fig 2C**)²⁵. Similar hairpin
84 structures are also found in viral SF2 helicases and they also seem to function as nucleic acid
85 duplex opener (**Fig 2DE**)^{26, 27}. Rather, DRAs contain accessory domains specialized for duplex

86 RNA recognition, including an insertion domain (HEL2i), a CTD, and additional motifs (Iic and
87 Vc) found in the helicase core (**Fig 1, 2A**)⁷. As a distinct group of macromolecular machines, the
88 mechanical functions of DRAs upon binding to RNA and ATP are related to other processes,
89 such as the release of signaling domains (CARDs of RIG-I) and activation of partner proteins
90 (MAVS).

91

92 **RIG-I: two-component molecular machine for sensing and responding to viral infections**

93 The RNA sensing process is the key step in the initiation of an antiviral innate immune
94 response. It is logical to think that selecting the correct RNA PAMPs rapidly and with high
95 fidelity would be required for a highly efficient host defense system. RIG-I has evolved to
96 comprise specific RNA recognition modules to handle this task (**Fig 1**). The CTD provides the
97 specificity for both the 5' triphosphate of RNA targets through electrostatic interactions, and for
98 the blunt ends of the RNA duplex through hydrophobic stacking to the first base pair (**Fig 1**)^{28, 29}.
99 The 5' triphosphate of the RNA establishes strong electrostatic interactions with the conserved
100 positively charged residues of RIG-I. This provides the structural basis for the high affinity and
101 specificity of RIG-I for the duplex RNAs bearing 5' triphosphates that are generated during viral
102 replication, as opposed to host RNAs generated during normal cellular metabolism (**Fig 1AB**).
103 The helicase domain displays specificity for the RNA duplex stem, albeit to a much lower extent
104 than the CTD-duplex end interaction (**Fig 1F**). Both the conserved helicase core and the HEL2i
105 domain, a novel insertion domain in HEL2 with five α -helices, contain specialized motifs that
106 allow RIG-I to bind the top or 5' strand of the RNA duplex (the conventional RNA-binding SF2
107 motifs interact with only the bottom or 3' tracking strand) (**Fig 1**). Interestingly, there are two
108 opposing functional surfaces on HEL2i: one RNA binding surface with a conserved residue

109 (Q511 in human RIG-I) that dynamically samples the RNA ligand (**Figs 1,3**)³⁰ and one inhibitory
110 surface that interacts with the CARD2 domain to maintain the auto-inhibited state of RIG-I⁵.
111 Thus, at the molecular level, HEL2i serves as a molecular transmitter, bridging the sensing and
112 signaling processes of RLRs (**Fig 3**).

113

114 **The CTD and the helicase domain act together in 5' triphosphorylated duplex RNA** 115 **recognition.**

116 These two RNA sensing modules are connected and coordinated by the pincer domain^{4,6}.
117 Unique to RLRs, this pincer domain is made of two long α helices, which emanate from the
118 HEL2 domain of the helicase core, stack back across the HEL1 domain and lead into the CTD
119 with a non-structured proline-rich linker^{4,6}. For 5' triphosphorylated substrates, RNA binding is
120 likely nucleated by duplex end capture mediated by an interaction between the triphosphate and
121 the CTD. Presumably, complete binding of the CTD:dsRNA terminus then brings the helicase
122 domain and duplex RNA stem into close proximity, effectively increasing their local
123 concentration and promoting their interaction. Alternatively, these two steps may be non-
124 sequential: in the *apo* enzyme, the RNA binding surfaces from both the CTD and the helicase
125 domains are well exposed and capable of simultaneous recognition of RNA PAMPs⁵. The length
126 and flexibility of the second pincer arm helps sandwich the duplex RNA between the CTD and
127 the HEL1 domain of the helicase core to form a hetero-molecular rigid body (**Figs 1,3**)⁶. The
128 HEL2 and HEL2i domains form a second rigid body, which displays significant degrees of
129 freedom across the RNA-free state, the RNA sensing state and the activated state of RIG-I (**Fig**
130 **3**). This design allows RIG-I to examine the correct chemistry and structure of the RNA ligand
131 ³⁰⁻³³.

132

133 **RIG-I prefers capping the ends of RNA duplex rather than binding internally.**

134 Like other RNA helicases, ATP binding closes the helicase core and subsequent
135 hydrolysis and product release allows cycling back to an open conformation (**Fig 1a, 3**). An
136 interpretation of this repetitive intra-molecular motion is that RIG-I may be able to translocate
137 along duplex RNA³⁴, allowing multiple copies of RIG-I to assemble and reside on a single
138 duplex RNA to provide stronger stimulatory signals for IFN production³⁴⁻³⁶. However, several
139 conflicting reports related to this proposed mechanism of RIG-I signaling still need to be
140 reconciled. First, in order for RIG-I to translocate along RNA duplex, the CTD must no longer
141 cap the RNA end and the high-affinity interaction between the CTD and the triphosphates must
142 be disrupted. Further, RIG-I also displays no intermolecular cooperativity for RNA binding,
143 prefers short RNA, including ten base pair hairpins and siRNA, for its enzymatic activity, and
144 can be effectively stimulated by short and long RNA with respect to IFN production³⁰. Finally, in
145 all known RIG-I:dsRNA complexes, RIG-I was crystallized at the ends of all RNA duplexes of
146 different length and sequence composition, even in the absence of the CTD domain (**Fig 3**),
147 further suggesting that RIG-I preferentially binds at the duplex RNA terminus. Therefore, it
148 seems plausible that the large conformational changes resulting from the intra-molecular
149 structural flexibility between the two rigid bodies of RIG-I (HEL1-dsRNA-CTD versus HEL2-
150 HEL2i) (**Fig 3**) coupled to cycles of ATP hydrolysis may provide an alternative explanation to
151 the results from the single molecule experiments by Myong et al., 2009 that were initially
152 interpreted to be RIG-I translocation.

153 Internal binding of the RNA duplex stem by RIG-I is not required for strong monomeric
154 binding at the 5' end³⁰. Indeed, our recent work allowed us to define the consensus, minimal

155 functional RNA PAMP for RIG-I. It is clear that RIG-I requires only the 5' terminus of duplex
156 RNA, along with an adjacent ten to twelve base pairs for binding (**Fig 1a**), ATP hydrolysis, and
157 cell-based IFN production³⁰. Interestingly, new evidence from EM studies in the Hur lab
158 suggests that, despite the lack of cooperativity, internal binding could be induced by a nucleation
159 effect initiated by RIG-I capping at the end of the RNA duplex which could lead to a more robust
160 interferon response^{35,36}. Conceivably, at lower concentrations of RIG-I in the resting state, RIG-
161 I surveys and binds only the ends of 5' trisphosphorylated RNA, but upon IFN induction and the
162 concomitant increase in cellular levels of RIG-I protein, RIG-I molecules may start to bind
163 internally near the RIG-I-capped RNA^{35,37}. A distinct conformation of RIG-I bound internally to
164 the duplex RNA is therefore highly desirable, which may provide a second – similar but not
165 identical – means to activate RIG-I. Carefully designed experiments are needed to further clarify
166 the functional implications of this RNA end capping preference versus the duplex internal
167 binding activity of RIG-I *in vivo*.

168

169 **The N-terminal CARDS of RIG-I turn on IFN production.**

170 The N-terminal tandem CARDS of RIG-I comprise the signaling domain (**Fig 4**), which
171 alone triggers robust IFN production when ectopically expressed in cells³⁸. The RIG-I CARDS,
172 specifically the first CARD domain – CARD1, turn on the intracellular signaling cascade by
173 interacting with the mono CARD domain of the mitochondrial adaptor protein MAVS and
174 inducing its oligomerization³⁹. In the resting cells of ducks, *apo* RIG-I adopts an auto-repressed
175 conformation in which CARD2 interacts with the HEL2i domain of the helicase⁵. This intra-
176 molecular inhibitory interaction locks the CARDS in an inaccessible conformation for MAVS
177 activation; a strategy that is likely employed in mammalian RIG-I as well^{5,38}. Both K63-linked

178 covalent ubiquitination and non-covalent polyubiquitin binding of the RIG-I CARDS have been
179 shown to mediate the MAVS activation process ¹⁶. Although the exact molecular mechanism is
180 unclear, ubiquitination and polyubiquitin binding might further rearrange the conformation of the
181 CARDS of RIG-I to promote CARD-CARD interactions between RIG-I and MAVS or might
182 facilitate RIG-I oligomerization (**Fig 4**)³⁶. It is thought that once MAVS oligomerizes and
183 recruits the downstream signaling kinases, the signaling cascade becomes essentially irreversible
184 ^{36, 39, 40}.

185

186 **Activation of RIG-I signaling is a carefully regulated process.**

187 Through the aforementioned molecular modules, RIG-I senses viral infection by binding
188 to the viral RNA PAMP and subsequently rearranges its conformation to initiate the intracellular
189 signaling cascade leading to IFN expression. IFNs then reset the body's metabolism and promote
190 both innate and adaptive immunity to defend against pathogens ⁴¹. This process is very costly
191 and often dangerous to the host; therefore it must be tightly regulated. RIG-I is such a well-
192 designed nano-mechanical device that it allows regulation at multiple levels. The auto-repressed
193 state sets the threshold for activation (**Fig 4**). The structural dynamics upon RNA binding and
194 sensing provides a means to examine the strength of the danger signal (**Fig 1a, 3**). The ATP
195 dependent conformational changes of the helicase domain switch off the auto-inhibition of the
196 CARDS ^{7, 42, 43}. Ubiquitin or phosphorylation mediated post-translational modifications further
197 potentiate RIG-I activation ^{16, 40, 44}. Lastly, multiple copies of activated RIG-I:RNA complex are
198 probably needed to activate the adaptor protein MAVS ⁴⁰.

199

200 **MDA5 (and LGP2) complements RIG-I in targeting a broad spectrum of viral infections.**

201 Despite the fact that MDA5 overlaps functionally with RIG-I, the two RLRs are not
202 entirely redundant when facing viral infections^{2,8}. Early RLR studies proposed RNA and length
203 preferences for MDA5 and RIG-I which helped to explain the ability of each RLR to detect
204 different but in some cases overlapping families of viruses^{2,8,45}. MDA5 shares the same protein
205 architecture and approximately 33% sequence identity with RIG-I. The number of structural
206 biology studies of MDA5 is catching up with those for RIG-I, providing us with insightful
207 comparisons between these two proteins, and allowing us to better understand the molecular
208 bases of their similarities and differences.

209

210 **Unlike RIG-I, MDA5 binds cooperatively to long RNA duplex.**

211 The cooperative binding of MDA5 to long RNA duplex molecules has been demonstrated
212 by biochemical, biophysical and structural methods⁴⁶⁻⁵⁰. This cooperativity is independent of the
213 CARDs and the interface has been mapped to HEL1 of one molecule of MDA5 and the CTD of
214 the neighboring molecule^{47,50}. This cooperativity is necessary for activation of MDA5, as
215 MDA5 displays poor cellular activity on short RNA species^{40,45,46}. The structure of MDA5
216 lacking the CARDs in complex with a 12mer RNA duplex exhibits several differences from
217 those of similar RIG-I:RNA complexes: first, the MDA5 CTD in the structure binds only to the
218 backbone of the RNA duplex but not to the end (**Fig 1**)⁵⁰; second, unlike the RIG-I CTD,
219 mutations that remove the RNA capping loop from the CTD of MDA5 do not weaken RNA
220 binding of MDA5⁵⁰. Therefore the respective CTDs of RIG-I and MDA5 play a major role in
221 distinguishing these proteins. Interestingly, encephalomyocarditis virus (EMCV), a *picornavirus*,
222 is recognized by MDA5 but not RIG-I, presumably because of the peptidyl modification at the 5'
223 end of the viral genome that would block RIG-I binding^{2,8}. In addition to differences in the

224 CTD, a HEL2 loop of MDA5 inserts in and widens the major groove of the RNA, whereas the
225 corresponding HEL2 loop of RIG-I actually resides near the dsRNA end.

226 Using EM reconstitution, Berke et al. revealed a helical envelop of MDA5 on an RNA
227 duplex⁴⁷. Interestingly, although the data were obtained for both full length and CARD-less
228 MDA5, the authors could not locate the CARDS⁴⁷. It is likely that in the activated MDA5:RNA
229 complex, the CARDS do not form a stable interaction with the HEL-CTD domains, but are
230 physically tethered to the HEL-CTD:RNA complex through the 100 amino acid long non-
231 structured linker between CARD2 and the HEL-CTD domains. The Hur group suggested that at
232 least 6-8 copies of the activated MDA5 (on a long duplex RNA of more than a hundred base
233 pairs) form the minimal activation unit – comprising a multimeric head-to-tail filament with the
234 free CARDS able to cluster together (**Fig 4**). This CARDS complex is then able to recruit MAVS
235 and trigger its oligomerization⁵⁰. This theory could explain the length preference of MDA5; a
236 longer RNA duplex is simply able to recruit and activate more copies of MDA5. However, this
237 putative CARDS complex as the initiator of the MDA5-mediated IFN activation requires further
238 study as the interface for self-association and the interface for MAVS interaction are not well-
239 defined at a structural level. In addition, like RIG-I, MDA5 also appears to require ubiquitination
240 or polyubiquitin binding for its function, most likely after MDA5 binds and oligomerizes on RNA
241 ^{40, 51, 52}.

242

243 **The structure and function of LGP2 is still poorly defined.**

244 As LGP2 lacks the N-terminal CARDS found in other RLRs, it likely retains no capacity
245 for signaling. Being able to bind dsRNA with its HEL-CTD structure might suggest a
246 mechanism of inhibition of RIG-I/MDA5 signaling^{10, 53, 54}. However, LGP2 knockout mice were

247 defective in responding to virus infection, particularly for picornaviruses like EMCV. Curiously,
248 synthetic RNAs (including polyIC) and *in vitro* transcribed RNAs elicited comparable IFN
249 production in both WT and LGP2^{-/-} mice^{9, 55}. Despite these contradictory results, LGP2 appears
250 to positively regulate MDA5 signaling through an as yet unclear mechanism while perhaps also
251 indirectly modulating RIG-I signaling^{9, 55, 46, 10, 53, 54}. Unfortunately, there is only one structure of
252 the LGP2 CTD in complex with a short RNA duplex (**Fig 1e**)⁵³, making it difficult to infer the
253 molecular basis of LGP2 function.

254 A recent structural study nicely demonstrated how paramyxovirus V protein selectively
255 inhibits MDA5 and LGP2⁵⁶. The viral protein actively disrupts the fold of the HEL2 domain of
256 MDA5, and consequently likely disrupts LGP2 based on protein sequence conservation analysis,
257 thereby impairing the RNA binding and ATP hydrolytic functions of both proteins⁵⁶. This
258 evasion strategy, while apparently specific for MDA5 and LGP2, may also indirectly act against
259 RIG-I through LGP2 via an undefined mechanism^{56, 57}.

260 Very little is known about how similar or different LGP2 is from RIG-I or MDA5 in
261 recognizing various RNA ligands. However, recently Bruns et al. demonstrated that robust basal
262 ATPase activity allows LGP2 to diversify its RNA recognition capacity⁵⁸. This result is
263 interesting in light of the fact that both RIG-I and MDA5 completely lack basal ATPase activity.
264 Moreover, the duck apo RIG-I structure suggests that ATP binding and hydrolysis can only
265 occur in the presence of RNA. Therefore, a structure of the apo and RNA bound LGP2 helicase
266 domain would help shed some light on this issue. Future *in vitro* and cellular studies will
267 hopefully answer how LGP2 recognizes RNA and whether its regulatory roles are performed by
268 directly acting on RIG-/MDA5. This will provide a clearer picture of LGP2 function in RLR
269 signaling.

270

271 **Conclusions and prospects**

272 Over the past few years, tremendous efforts have been invested in better understanding
273 the molecular biology of RLRs and in attempting to answer several important questions: How do
274 RLRs sense viral infection? What are the PAMPs of RLRs? What is the activation mechanism?
275 How is the downstream signaling cascade activated for the production of IFN? What are the
276 similarities and differences between RLRs, across cell types, tissues, and species? How do
277 viruses counter RLR recognition and response? What are the potential therapeutic applications in
278 targeting the RLR systems for antivirals, vaccines, and anticancer drugs? Moving forward, there
279 are still plenty of interesting and urgent questions that need to be addressed in the studies of
280 RLRs and more generally in host-and-pathogen interactions. Here are some unanswered
281 questions about the RLR activation pathway (**Fig 4**): (1) What is/are the conformation (s) of
282 RIG-I binding internally to dsRNA? And what is the relationship between the internally bound
283 RIG-I versus end-capped RIG-I? How are they different in their activation mechanism? (2) What
284 is the *apo* state of MDA5? Is RNA binding alone able to activate MDA5? What is the function of
285 ATP in MDA5 activation? Can RIG-I and MDA5 work together on the same RNA in the same
286 subcellular environment?(3) What are the minimum copies of activated RIG-I for initiating
287 MAVS oligomerization? (4) How are the CARDS of RIG-I and MDA5 different from each other?
288 What are the 3D molecular rearrangements of CARDS for turning on the MAVS oligomerization.
289 (5) What is the molecular basis of the ubiquitination/polyubiquitin binding in RIG-I and/or
290 MDA5 activation process? (6) What are the 3D molecular rearrangements of the MAVS fiber on
291 the mitochondria membrane? How does this fiber turn on the downstream signaling effectors? (7)
292 What is the molecular role of LGP2 in RLR mediated antiviral immune response ?

293

294

295 **Acknowledgements**

296 The author would like to thank Dr Andrew S. Kohlway, David C. Rawling, and Dr Katja Fink
297 for their critical reading of the manuscript.

298 **Conflict of Interest**

299 The author declares no competing financial interests.

300 **References**

- 301 1. Takeuchi O, Akira S. Pattern recognition receptors and inflammation. *Cell* 2010; 140:805-20.
302 2. Ramos HJ, Gale M, Jr. RIG-I Like Receptors and Their Signaling Crosstalk in the Regulation of
303 Antiviral Immunity. *Curr Opin Virol* 2011; 1:167-76.
304 3. Fujita T, Onoguchi K, Onomoto K, Hirai R, Yoneyama M. Triggering antiviral response by RIG-I-
305 related RNA helicases. *Biochimie* 2007; 89:754-60.
306 4. Jiang F, Ramanathan A, Miller MT, Tang GQ, Gale M, Jr., Patel SS, et al. Structural basis of RNA
307 recognition and activation by innate immune receptor RIG-I. *Nature* 2011; 479:423-7.
308 5. Kowalinski E, Lunardi T, McCarthy AA, Louber J, Brunel J, Grigorov B, et al. Structural basis for
309 the activation of innate immune pattern-recognition receptor RIG-I by viral RNA. *Cell* 2011; 147:423-35.
310 6. Luo D, Ding SC, Vela A, Kohlway A, Lindenbach BD, Pyle AM. Structural insights into RNA
311 recognition by RIG-I. *Cell* 2011; 147:409-22.
312 7. Luo D, Kohlway A, Pyle AM. Duplex RNA activated ATPases (DRAs): platforms for RNA sensing,
313 signaling and processing. *RNA Biol* 2013; 10:111-20.
314 8. Schlee M. Master sensors of pathogenic RNA - RIG-I like receptors. *Immunobiology* 2013.
315 9. Satoh T, Kato H, Kumagai Y, Yoneyama M, Sato S, Matsushita K, et al. LGP2 is a positive regulator
316 of RIG-I- and MDA5-mediated antiviral responses. *Proc Natl Acad Sci U S A* 2010; 107:1512-7.
317 10. Komuro A, Horvath CM. RNA- and virus-independent inhibition of antiviral signaling by RNA
318 helicase LGP2. *J Virol* 2006; 80:12332-42.
319 11. Loo YM, Gale M, Jr. Immune signaling by RIG-I-like receptors. *Immunity* 2011; 34:680-92.
320 12. Xu LG, Wang YY, Han KJ, Li LY, Zhai Z, Shu HB. VISA is an adapter protein required for virus-
321 triggered IFN-beta signaling. *Mol Cell* 2005; 19:727-40.
322 13. Seth RB, Sun L, Ea CK, Chen ZJ. Identification and characterization of MAVS, a mitochondrial
323 antiviral signaling protein that activates NF-kappaB and IRF 3. *Cell* 2005; 122:669-82.
324 14. Meylan E, Curran J, Hofmann K, Moradpour D, Binder M, Bartenschlager R, et al. Cardif is an
325 adaptor protein in the RIG-I antiviral pathway and is targeted by hepatitis C virus. *Nature* 2005;
326 437:1167-72.
327 15. Kawai T, Takahashi K, Sato S, Coban C, Kumar H, Kato H, et al. IPS-1, an adaptor triggering RIG-I-
328 and Mda5-mediated type I interferon induction. *Nat Immunol* 2005; 6:981-8.
329 16. Oshiumi H, Matsumoto M, Seya T. Ubiquitin-mediated modulation of the cytoplasmic viral RNA
330 sensor RIG-I. *J Biochem* 2012; 151:5-11.
331 17. Wies E, Wang MK, Maharaj NP, Chen K, Zhou S, Finberg RW, et al. Dephosphorylation of the
332 RNA sensors RIG-I and MDA5 by the phosphatase PP1 is essential for innate immune signaling. *Immunity*
333 2013; 38:437-49.
334 18. Kawai T, Akira S. Antiviral signaling through pattern recognition receptors. *J Biochem* 2007;
335 141:137-45.
336 19. Seth RB, Sun L, Chen ZJ. Antiviral innate immunity pathways. *Cell Res* 2006; 16:141-7.
337 20. Medzhitov R, Janeway CA, Jr. Innate immunity: impact on the adaptive immune response.
338 *Current opinion in immunology* 1997; 9:4-9.
339 21. Takeuchi O, Akira S. Innate immunity to virus infection. *Immunol Rev* 2009; 227:75-86.
340 22. Liu S, Chen J, Cai X, Wu J, Chen X, Wu YT, et al. MAVS recruits multiple ubiquitin E3 ligases to
341 activate antiviral signaling cascades. *eLife* 2013; 2:e00785.
342 23. Pyle AM. Translocation and Unwinding Mechanisms of RNA and DNA Helicases. *Annual Review*
343 *of Biophysics* 2008; 37:317-36.
344 24. Fairman-Williams ME, Guenther UP, Jankowsky E. SF1 and SF2 helicases: family matters. *Curr*
345 *Opin Struct Biol* 2010; 20:313-24.

346 25. Buttner K, Nehring S, Hopfner KP. Structural basis for DNA duplex separation by a superfamily-2
347 helicase. *Nat Struct Mol Biol* 2007; 14:647-52.

348 26. Gu M, Rice CM. Three conformational snapshots of the hepatitis C virus NS3 helicase reveal a
349 ratchet translocation mechanism. *Proc Natl Acad Sci U S A* 2010; 107:521-8.

350 27. Luo D, Xu T, Watson RP, Scherer-Becker D, Sampath A, Jahnke W, et al. Insights into RNA
351 unwinding and ATP hydrolysis by the flavivirus NS3 protein. *EMBO J* 2008; 27:3209-19.

352 28. Wang Y, Ludwig J, Schuberth C, Goldeck M, Schlee M, Li H, et al. Structural and functional
353 insights into 5'-ppp RNA pattern recognition by the innate immune receptor RIG-I. *Nat Struct Mol Biol*
354 2010; 17:781-7.

355 29. Lu C, Xu H, Ranjith-Kumar CT, Brooks MT, Hou TY, Hu F, et al. The structural basis of 5'
356 triphosphate double-stranded RNA recognition by RIG-I C-terminal domain. *Structure* 2010; 18:1032-43.

357 30. Kohlway A, Luo D, Rawling DC, Ding SC, Pyle AM. Defining the functional determinants for RNA
358 surveillance by RIG-I. *EMBO Rep* 2013; 14:772-9.

359 31. Vela A, Fedorova O, Ding SC, Pyle AM. The thermodynamic basis for viral RNA detection by the
360 RIG-I innate immune sensor. *J Biol Chem* 2012; 287:42564-73.

361 32. Schmidt A, Schwerd T, Hamm W, Hellmuth JC, Cui S, Wenzel M, et al. 5'-triphosphate RNA
362 requires base-paired structures to activate antiviral signaling via RIG-I. *Proc Natl Acad Sci U S A* 2009;
363 106:12067-72.

364 33. Schlee M, Roth A, Hornung V, Hagmann CA, Wimmenauer V, Barchet W, et al. Recognition of 5'
365 triphosphate by RIG-I helicase requires short blunt double-stranded RNA as contained in panhandle of
366 negative-strand virus. *Immunity* 2009; 31:25-34.

367 34. Myong S, Cui S, Cornish PV, Kirchhofer A, Gack MU, Jung JU, et al. Cytosolic viral sensor RIG-I is a
368 5'-triphosphate-dependent translocase on double-stranded RNA. *Science* 2009; 323:1070-4.

369 35. Patel JR, Jain A, Chou YY, Baum A, Ha T, Garcia-Sastre A. ATPase-driven oligomerization of RIG-I
370 on RNA allows optimal activation of type-I interferon. *EMBO Rep* 2013; 14:780-7.

371 36. Peisley A, Wu B, Yao H, Walz T, Hur S. RIG-I Forms Signaling-Competent Filaments in an ATP-
372 Dependent, Ubiquitin-Independent Manner. *Mol Cell* 2013; 51:573-83.

373 37. Goulet ML, Olagnier D, Xu Z, Paz S, Belgnaoui SM, Lafferty EI, et al. Systems analysis of a RIG-I
374 agonist inducing broad spectrum inhibition of virus infectivity. *PLoS Pathog* 2013; 9:e1003298.

375 38. Yoneyama M, Kikuchi M, Natsukawa T, Shinobu N, Imaizumi T, Miyagishi M, et al. The RNA
376 helicase RIG-I has an essential function in double-stranded RNA-induced innate antiviral responses. *Nat*
377 *Immunol* 2004; 5:730-7.

378 39. Hou F, Sun L, Zheng H, Skaug B, Jiang QX, Chen ZJ. MAVS forms functional prion-like aggregates
379 to activate and propagate antiviral innate immune response. *Cell* 2011; 146:448-61.

380 40. Jiang X, Kinch LN, Brautigam CA, Chen X, Du F, Grishin NV, et al. Ubiquitin-induced
381 oligomerization of the RNA sensors RIG-I and MDA5 activates antiviral innate immune response.
382 *Immunity* 2012; 36:959-73.

383 41. Pestka S. The interferons: 50 years after their discovery, there is much more to learn. *J Biol*
384 *Chem* 2007; 282:20047-51.

385 42. Luo D, Kohlway A, Vela A, Pyle AM. Visualizing the determinants of viral RNA recognition by
386 innate immune sensor RIG-I. *Structure* 2012; 20:1983-8.

387 43. Kolakofsky D, Kowalinski E, Cusack S. A structure-based model of RIG-I activation. *RNA* 2012;
388 18:2118-27.

389 44. Kato H, Takahashi K, Fujita T. RIG-I-like receptors: cytoplasmic sensors for non-self RNA. *Immunol*
390 *Rev* 2011; 243:91-8.

391 45. Kato H, Takeuchi O, Sato S, Yoneyama M, Yamamoto M, Matsui K, et al. Differential roles of
392 MDA5 and RIG-I helicases in the recognition of RNA viruses. *Nature* 2006; 441:101-5.

- 393 46. Peisley A, Jo MH, Lin C, Wu B, Orme-Johnson M, Walz T, et al. Kinetic mechanism for viral dsRNA
394 length discrimination by MDA5 filaments. *Proc Natl Acad Sci U S A* 2012.
- 395 47. Berke IC, Yu X, Modis Y, Egelman EH. MDA5 assembles into a polar helical filament on dsRNA.
396 *Proc Natl Acad Sci U S A* 2012; 109:18437-41.
- 397 48. Berke IC, Modis Y. MDA5 cooperatively forms dimers and ATP-sensitive filaments upon binding
398 double-stranded RNA. *Embo J* 2012; 31:1714-26.
- 399 49. Peisley A, Lin C, Wu B, Orme-Johnson M, Liu M, Walz T, et al. Cooperative assembly and dynamic
400 disassembly of MDA5 filaments for viral dsRNA recognition. *Proc Natl Acad Sci U S A* 2011; 108:21010-5.
- 401 50. Wu B, Peisley A, Richards C, Yao H, Zeng X, Lin C, et al. Structural Basis for dsRNA Recognition,
402 Filament Formation, and Antiviral Signal Activation by MDA5. *Cell* 2013; 152:276-89.
- 403 51. Zeng W, Sun L, Jiang X, Chen X, Hou F, Adhikari A, et al. Reconstitution of the RIG-I pathway
404 reveals a signaling role of unanchored polyubiquitin chains in innate immunity. *Cell* 2010; 141:315-30.
- 405 52. Gack MU, Shin YC, Joo CH, Urano T, Liang C, Sun L, et al. TRIM25 RING-finger E3 ubiquitin ligase
406 is essential for RIG-I-mediated antiviral activity. *Nature* 2007; 446:916-20.
- 407 53. Li X, Ranjith-Kumar CT, Brooks MT, Dharmiah S, Herr AB, Kao C, et al. The RIG-I-like receptor
408 LGP2 recognizes the termini of double-stranded RNA. *J Biol Chem* 2009; 284:13881-91.
- 409 54. Murali A, Li X, Ranjith-Kumar CT, Bhardwaj K, Holzenburg A, Li P, et al. Structure and function of
410 LGP2, a DEX(D/H) helicase that regulates the innate immunity response. *J Biol Chem* 2008; 283:15825-
411 33.
- 412 55. Venkataraman T, Valdes M, Elsby R, Kakuta S, Caceres G, Saijo S, et al. Loss of DEXD/H box RNA
413 helicase LGP2 manifests disparate antiviral responses. *J Immunol* 2007; 178:6444-55.
- 414 56. Motz C, Schuhmann KM, Kirchhofer A, Moldt M, Witte G, Conzelmann KK, et al. Paramyxovirus V
415 proteins disrupt the fold of the RNA sensor MDA5 to inhibit antiviral signaling. *Science* 2013; 339:690-3.
- 416 57. Childs K, Randall R, Goodbourn S. Paramyxovirus V proteins interact with the RNA Helicase LGP2
417 to inhibit RIG-I-dependent interferon induction. *J Virol* 2012; 86:3411-21.
- 418 58. Bruns AM, Pollpeter D, Hadizadeh N, Myong S, Marko JF, Horvath CM. ATP hydrolysis enhances
419 RNA recognition and antiviral signal transduction by the innate immune sensor, laboratory of genetics
420 and physiology 2 (LGP2). *J Biol Chem* 2013; 288:938-46.
- 421 59. Bono F, Ebert J, Lorentzen E, Conti E. The crystal structure of the exon junction complex reveals
422 how it maintains a stable grip on mRNA. *Cell* 2006; 126:713-25.
- 423 60. Andersen CB, Ballut L, Johansen JS, Chamieh H, Nielsen KH, Oliveira CL, et al. Structure of the
424 exon junction core complex with a trapped DEAD-box ATPase bound to RNA. *Science* 2006; 313:1968-72.

425

426 **Figure Captions:**

427 **Figure 1. Molecular features of RNA recognition by RLRs.** (A) Schematic view of the RLR
428 genes (upper panel) and the RIG-I:dsRNA interface (lower panel). The HEL2 and HEL2i
429 domains are connected as one rigid body and move along the RNA, which is presumably
430 regulated by the ATP binding and hydrolysis state of the protein. The HEL1-dsRNA-CTD forms
431 another sandwich like rigid body, capping the blunt end of the duplex RNA. (B) The CTD of
432 RIG-I is responsible for the recognition of the blunt end of dsRNA. The 5' triphosphate group of
433 the RNA specifically interacts with the conserved positively charged residues on the CTD. Color
434 codes: PDB-4AY2 in red, 3LRR in green, 3LRN in magenta, and 3NCU in blue. (C)
435 Electrostatic surface view of the RIG-I CTD, highlighting the mode of RNA-protein interaction:
436 the positively charged pocket for RNA 5' triphosphate group recognition and RNA end capping.
437 (D) Electrostatic surface view of the MDA5 CTD, highlighting the mode of RNA-protein
438 interaction: the positive patch for RNA backbone recognition and the absence of RNA end
439 capping. (E) Electrostatic surface view of the LGP2 CTD. Although the dsRNA end is still
440 capped, there is no positively charged surface at the 5' end of the dsRNA. (F) Electrostatic
441 surface view of the duck RIG-I helicase domain in complex with a synthetic 19 mer RNA duplex
442 and an ATP analog (PDB:4A36). The helicase domain is in the most closed conformation and
443 RIG-I binds at the end of RNA duplex.

444
445 **Figure 2. Structural features of the Superfamily 2 helicases.** (A) RIG-I:dsRNA interaction.
446 Duplex RNA remains base paired. The HEL2i domain, instead of separating the duplex, interacts
447 with the dsRNA backbone^{4,6}. (B) DEAD-box RNA helicase eIF4A3 binds to the single stranded
448 RNA^{59,60}. (C) Archaeal Hel308 DNA helicase separates the DNA duplex with the beta-hairpin
449 insertion in red on the helicase domain 2²⁵. (D) HCV NS3 helicase binds to the single stranded
450 DNA and the beta-hairpin insertion on the helicase domain 2 prevents the complementary strand
451 from basepairing with the single stranded nucleic acid²⁶. (E) Dengue NS3 helicase binds to the
452 single stranded RNA. Similarly, the beta-hairpin insertion on the helicase domain 2 is thought to
453 function as the RNA duplex opener²⁷. The helicase core domains 1 and 2 are colored in wheat
454 yellow, the HEL2i domain or the beta-hairpin insertion in red, nucleic acids in magenta, and the
455 accessory domains are in gray.

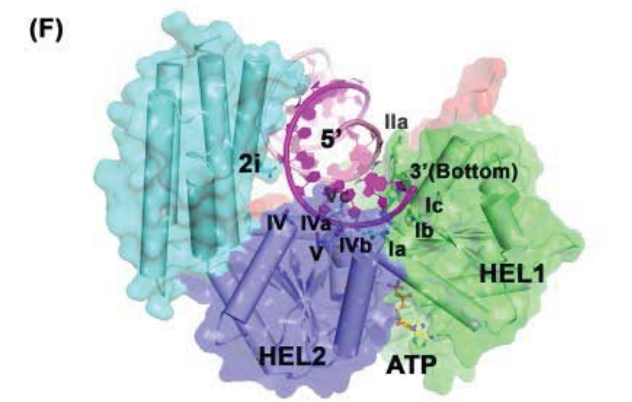
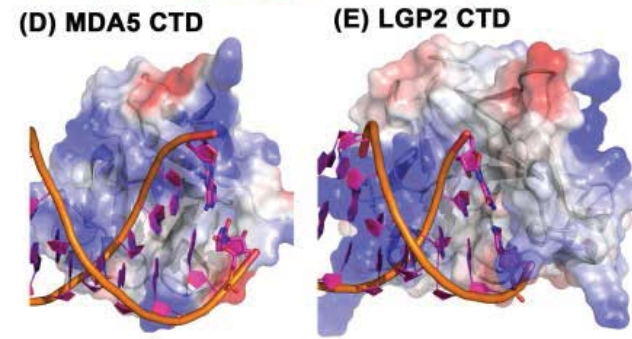
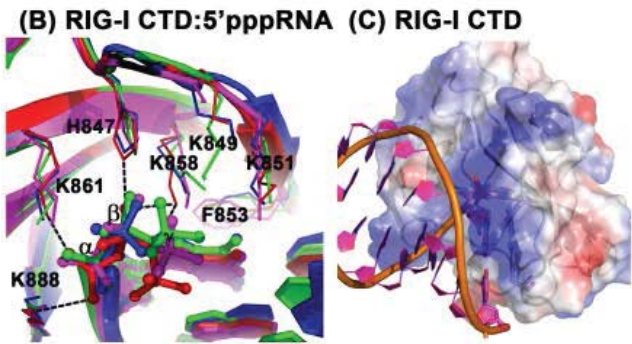
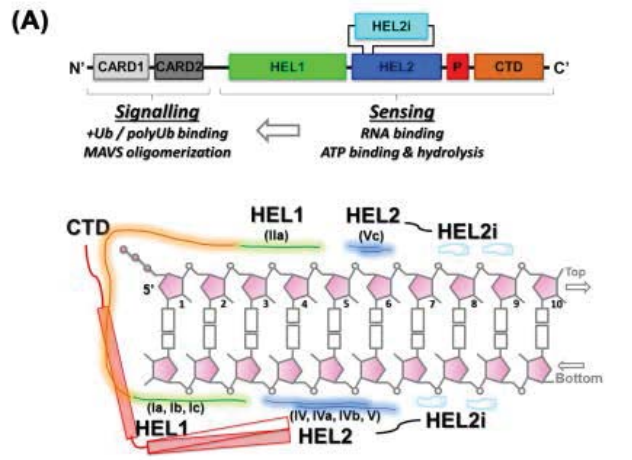
456
457 **Figure 3. Superposition of the RIG-I structures.** (A) Alignment of the RIG-I structures based
458 on the HEL1 domain. The structures highlight that HEL2-HEL2i as a rigid domain moving
459 relative to the HEL1-dsRNA-CTD tri-party fold. (B) Top view of the aligned structures. Left:
460 relative locations of the HEL2i domain and dsRNA. Right: relative locations of the HEL2i
461 domain and CTD. (C) A model of the relative HEL2i locations (solid circles) in RIG-I structure
462 as an indicator for the gating mechanism of RIG-I activation. The figure is a schematic
463 representation of the HEL2i motions (the yellow trajectory that goes through the center of the
464 circles) shown in (B) with the same color codes. In the resting cells, RIG-I remains in the sensing
465 state where the HEL2i domain does not interact with the RNA, as indicated in the *apo* RIG-I

466 structures 3TBK (black), 4A2W (dark gray), and 4A2Q (light gray). At the checkpoint state
467 (dashline), RIG-I encounters foreign RNA species and the HEL2i domain participates in the
468 RNA recognition process as indicated in the RIG-I RNA complexes 3ZD6 (cyan), 2YKG (blue)
469 and 3ZD7 (light blue). Effective activation of RIG-I requires additional trigger by ATP to disrupt
470 the HEL2i-CARD2 interaction as indicated in the ternary complexes of RIG-I, RNA and ATP
471 analogs, 3TMI (pink) and 4A36 (red).

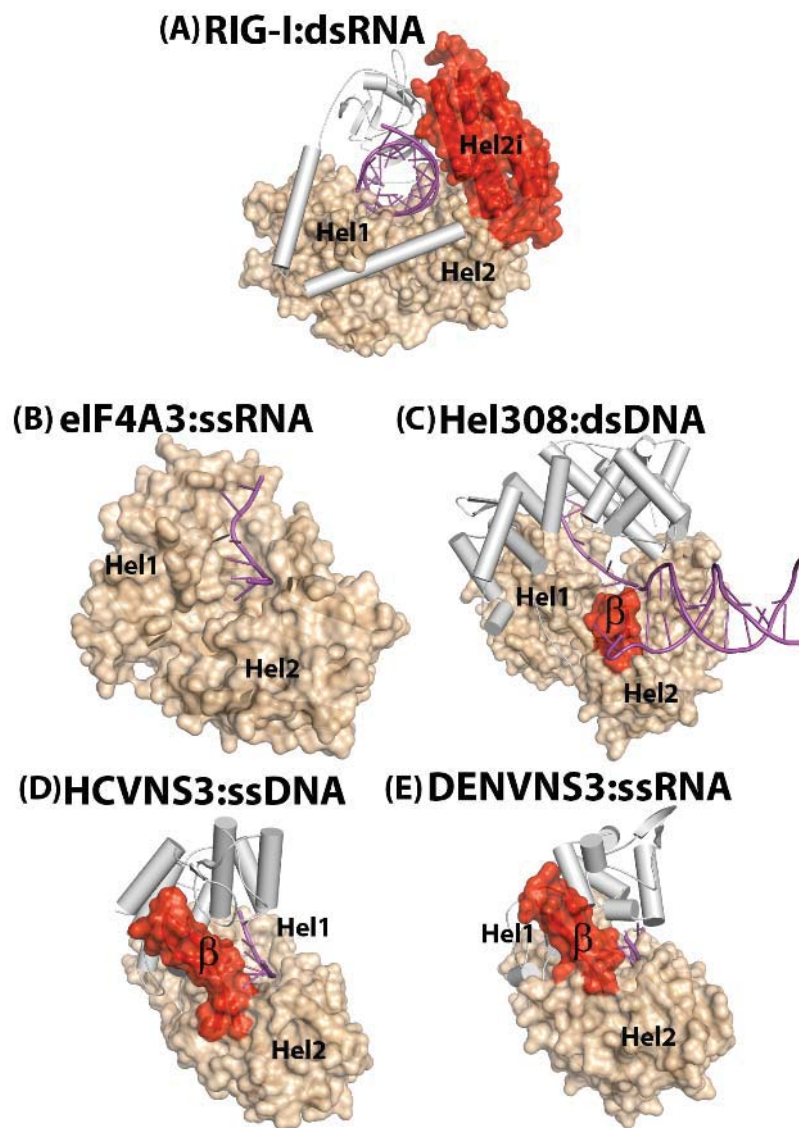
472
473 **Figure 4. Current opinions on the molecular basis of the RLR signaling pathway. (A) RNA**
474 **sensing and activation of RIG-I (B) RNA sensing and activation of MDA5.** All the crystal
475 structures of RIG-I reside at the end of the duplex RNA, at least suggesting RIG-I prefers RNA
476 ends, while MDA5 has been shown to bind RNA duplex internally and oligomerizes
477 cooperatively on long duplex RNA. Ubiquitination and polyubiquitin chain non-covalent binding
478 to the RIG-I CARDS are essential for RIG-I activation, which presumably occurs downstream of
479 the molecular events of RNA binding and ATP binding to RIG-I. MAVS resides on the outer
480 membrane of mitochondria and is activated by the RIG-I or MDA5 CARDS through the
481 formation of fiber-like high order oligomers. This leads to the activation of IFN production
482 through the NFkB and IRF3 signaling pathway.

483

484 Figures
 485 Figure 1.

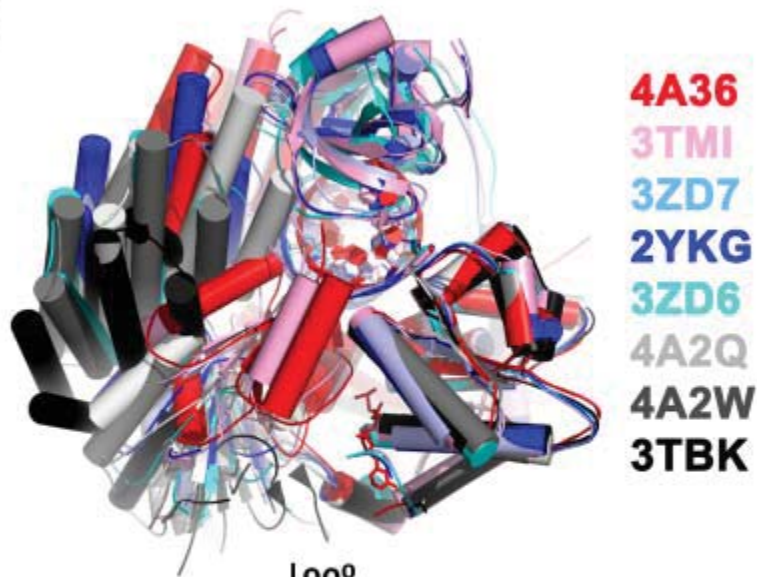


486

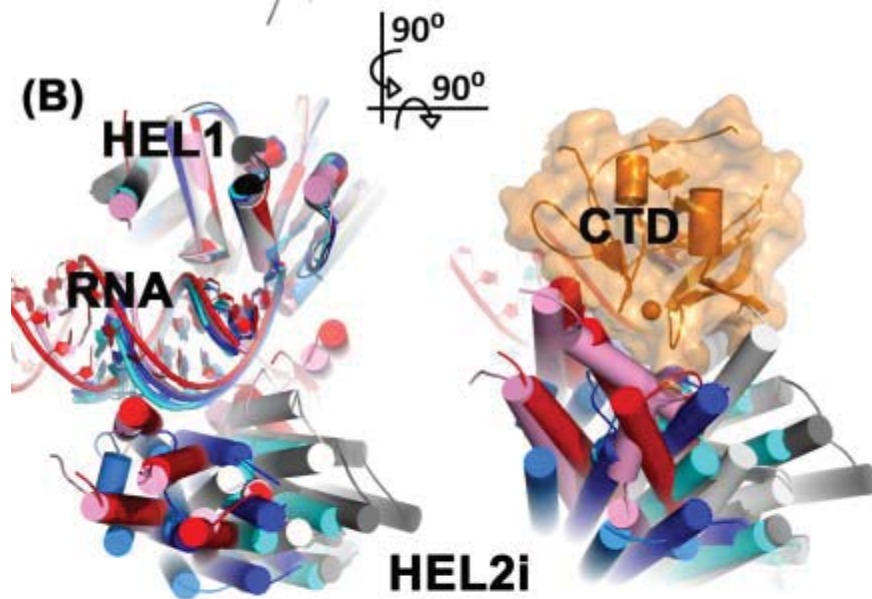


488
489
490
491

(A)



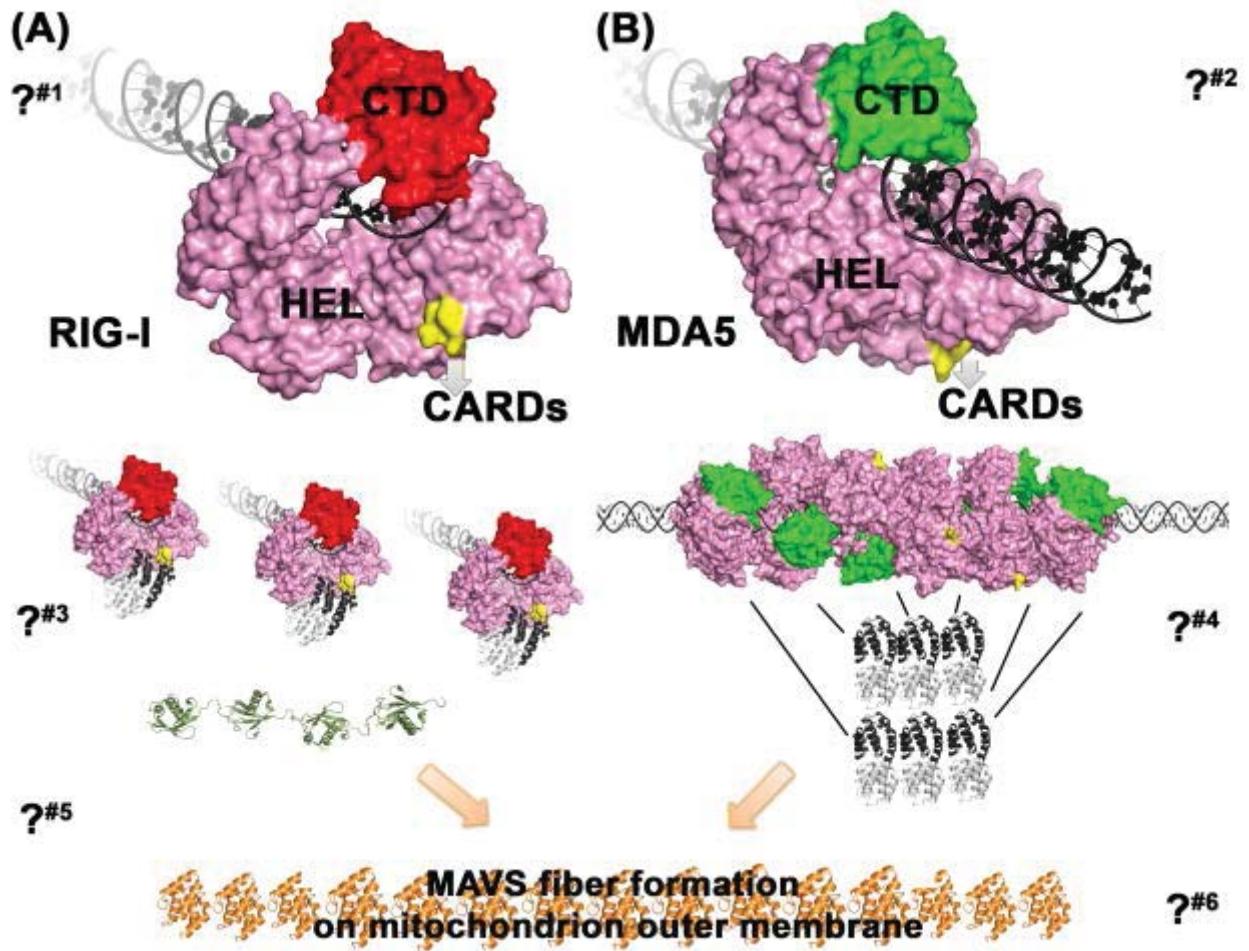
(B)



(C)



494 Figure 4.



495
496
497
498